ABHINAV
NATIONAL MONTHLY REFEREED JOURNAL OF RESEARCH IN SCIENCE & TECHNOLOGY
www.abhinavjournal.com

THE GROWTH OF AL-DOPED ZnO VIA SOLID-STATE CHEMICAL VAPOR DEPOSITION

Dr. L.S. Chuah[1], S. S. Tneh[2] and Dr. Z. Hassan[3]

[1]Professor, Physics Section, School of Distance Education, University Sains Malaysia, Penang, Malaysia
Email: chuahleesiang@yahoo.com
[2]Research Scholar, School of Physics, University Sains Malaysia, Penang, Malaysia
Email: sstneh@yahoo.com
[3]Professor, School of Physics, University Sains Malaysia, Penang, Malaysia
Email: zai@yahoo.com

ABSTRACT

To the best of our knowledge, this is the first time that Al-doped ZnO films grown by solid-state chemical vapor deposition (SSCVD) have been reported. Al-doped ZnO films have been synthesized on p-type silicon substrates by solid-source chemical vapor deposition using $AlCl_3$ (99%) and $Zn(O_2CCH_3)_2(H_2O)_2$ (99%) as the precursor. This is the first time that $AlCl_3$ has been introduced as dopant source. The XRD patterns of nanostructure films reveal the crystalline behavior and are hexagonal structure. Observations of the microstructure of Al-doped ZnO were performed by scanning electron microscopy (SEM). The structure of the films persisted unchanged by doping. The influence of doping on the optical characteristics of the films was studied. Blue shift of the band gap because of the doping is perceived. This recognized blue shift designates an improve in the band gap and is related to the Burstein-Moss influence.

Keywords: Al-doped, ZnO, Thin Film, Si, CVD

INTRODUCTION

Zinc oxide (ZnO) is an n-type metal oxide with a wide energy (3.6 eV) bandgap, which has been intensively investigated for utilizations for example varistor, sensors and electrodes [1-3]. In particular, n-type semiconductors for example SnO_2, TiO_2, and Fe_2O_3 have extensively been applied for the detection various toxic gases for example H_2, CO, CH_4, NO, and alcohol [4-8].

Doping is basic to restraint the characteristics of the semiconductors and to get new multifunctional materials. When ZnO films are doped with the suitable metal atoms, for example Al, Cd, Sn, Ga, In, their conductivity can be altered from values as low as 10^{-10} $(\Omega\ cm)^{-1}$ to values as high as 10^4 $(\Omega\ cm)^{-1}$. The wide range of conductivities and conductivity alters upon various environmental situations make ZnO films suitable materials for oxidant gas sensing layers [9–11]. Dopant occupancy ascertains notable changes of film physical characterizes as crystal structure, surface morphological, optical characteristics (associated with photoconductivity) which reveal directly on film sufficiency to perform as a sensing layer [12, 13]. In addition, doped ZnO has many advantages over indium tin oxide (ITO) involving low cost, non-toxicity, which make it an assuring nominee material for transparent conducting oxide of silicon thin film solar cells.

A variety method has been applied to synthesis aluminum-doped zinc oxide (AZO) thin films. These comprise chemical vapor deposition (CVD), reactive thermal vacuum evaporation, sol-gel, magnetron sputtering, spray pyrolysis, and pulsed laser deposition (PLD). In comparison with these techniques, CVD has many advantages for example (i) can be deposited with very high purity, (ii) high deposition rates, (iii) simplicity, and (iv) capability to grow films at a low process temperature [14-19]. Solid state chemical vapor deposition (SSCVD) is a beneficial approach for the synthesis of films, contributing the choice of yielding good quality films, larger area uniformity, and availability of various ambient in situ doping processes.

In this paper, we will present the development of microstructural characteristics of the Al-doped ZnO grown onto the p-type Si substrates using solid state chemical vapor deposition (SSCVD) method. Their characterizations using X-ray diffraction (XRD), and optical and transport measurements. Crystallinity quality and surface morphology of the ZnO films were correlated with their optical properties.

EXPERIMENT

Al-doped ZnO films have been synthesized on p-type silicon substrate by solid-source chemical vapor deposition. $AlCl_3$ (99%) and $Zn(O_2CCH_3)_2(H_2O)_2$ (99%) were used as the precursor and air from atmospheric as the oxygen source. The boat was loaded into a furnace. The source temperature and substrate temperature fixed at 430°C. The deposition time was 2 min. After the furnace cooled down to room temperature naturally, silicon substrates were removed for inspection.

The surface morphology of samples was studied utilizing a scanning electron microscope operating at low voltage (15kV) to minimize charging effects. SEM digitized micrographs were obtained with a magnification 30,000 X. The structural properties of the as-grown Al-doped ZnO films were investigated by X-ray diffraction (XRD) with Cu Kα radiation. The optical transmittance spectra for Al-doped ZnO films were recorded using a UV-Visible spectrophotometer in the range of 300-800 nm.

Firstly, gold (Au) with 200 nm thickness was sputtered onto the ZnO thin film through a metal mask, followed by 200 nm capping layer of nickel (Ni) with thermal evaporator. For the measurement of electrical properties, the current-voltage (*I-V*) characteristics were measured by using high-voltage source/measure unit [20]. The applied voltage was varied from 0 to 10 V.

RESULTS AND DISCUSSION

From figure 1, the XRD patterns of the Al-doped ZnO thin film on p-type Si (111) reveal reflection from the (100), (002), (101), and (110) planes of ZnO for 2θ values of 26.7°, 34.0°, 38.1°, 51.9° and 65.4°, respectively. The Al-doped ZnO films displayed polycrystalline hexagonal structure. For Al-ZnO on p-Si , we obtained amorphous ZnO. No metallic zinc (Zn) or aluminium (Al) characteristic peaks are detected. No signal of their oxides can be viewed, which is related to the good crystal formation of the ZnO films during deposition. For Al-doped ZnO, the intensities of (100) and (101) planes are less than the intensity of (002) planes indicating the preferred grain growth along the (002) plane.

For estimate the particle size of the deposited films, the Debye-Scherrer formula was used on the XRD pattern of the doped ZnO thin films which is given as $d = (0.9\lambda / \beta \cos \theta)$ where, λ is the wavelength of the X-ray employed which in this case is 0.15418 nm for Cu-kα. β is the FWHM (full width at half maximum) and θ is the usual Bragg's angle (deg) [21-24]. Estimating '*d*' from the premium two XRD patterns, it has been detected that the mean particle thickness of the prepared Al-doped films on Si(111) is about 38.0 nm.

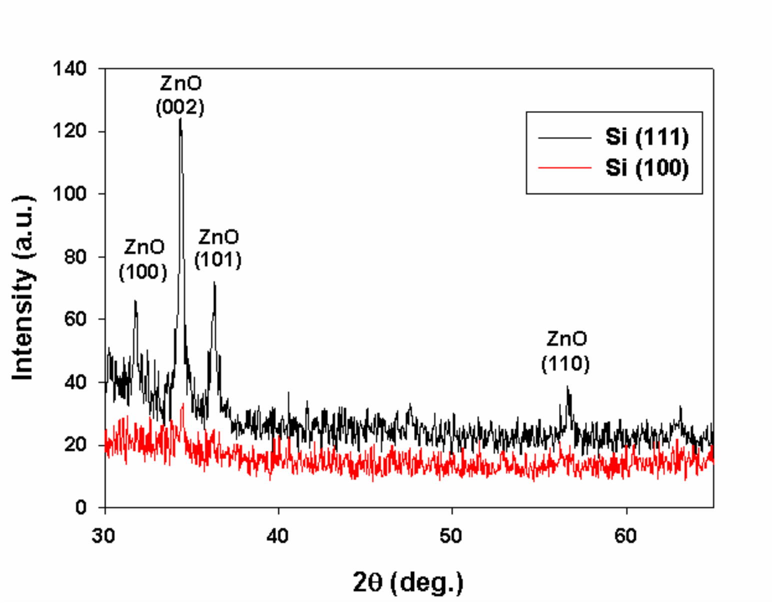

Fig.1. X-ray diffraction patterns of the Al-doped ZnO films

Surface morphologies gained throughout Scanning Electron Microscope (SEM) of Al-doped ZnO films are revealed in Figure 2. It can be seen that both SEM have same grains size. The optical transmittance (300-800nm) spectra for undoped and Al-doped as deposited ZnO films are shown in Figure 3. All the data are collected at room temperature. It can be seen that average optical transmittance in the visible light wavelength range which is vital for its utilizations for example transparent conductive films and solar cell windows. The low transmittance for the undopes and Al-doped ZnO films could be because of the excess Zn ions exist in the interstitial sites and they absorb light. The absorption edges for the Al-doped ZnO films shift towards lower wavelengths compared with that of the undoped sample. This observed blue shift represents an increase in the band gap and is related to the Burstein-Moss effect. According to the Burstein–Moss effect, the increase of the Fermi level in the conduction band leads to the bandgap energy broadening with increasing carrier concentration [25]. Assuming the absorption coefficient corresponding to the direct band gap of the wurtzite structure, we have made a plot of $(\alpha^* (hv))^2$ against the energy *hv* (see Figure 4). The values of optical band gap energies E_g were obtained by extrapolating the straight portion to the $h\upsilon$ axis at $(\alpha h\upsilon) = 0$. The obvious absorption edge can be precisely confirmed for the high quality films by the linear fit.

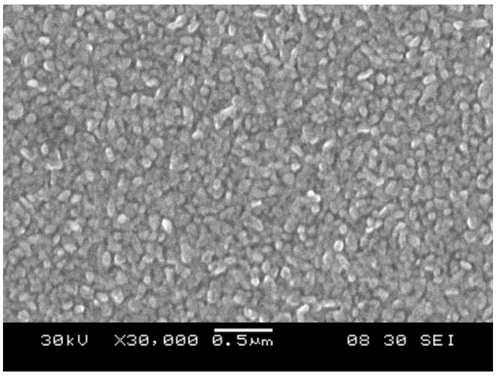

(a) Al-doped ZnO on p-Si(111)

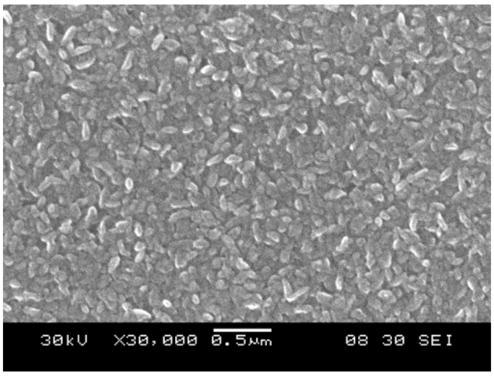

(b) Al-doped ZnO on p-Si(100)

Fig.2. SEM images of Al-doped ZnO thin films on silicon substrate. Magnification was 30 kX and accelerating voltage was 30kV for the SEM measurements

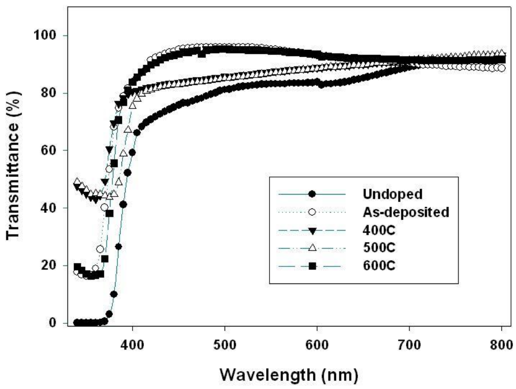

Fig.3. The optical transmittance spectra for undoped, as deposited, and annealed Al-doped ZnO films

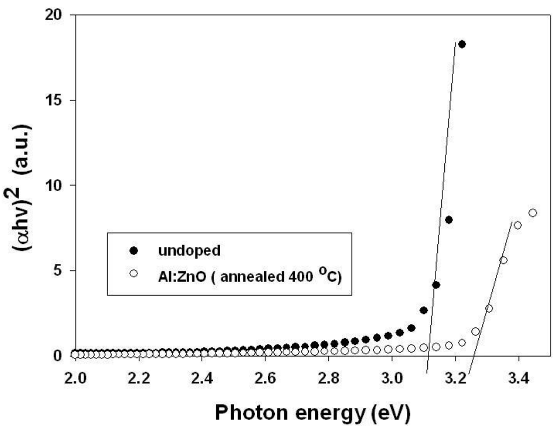

Fig.4. Optical transmittance spectrum of the pure ZnO and Al doped ZnO thin films

Figure 5 shows typical I-V characteristics of Au/Ni on Al-doped ZnO/p-Si(111) films as a function of the annealing temperature. All samples showed rectifying I-V characteristics. Nevertheless, the IV curves enhanced with increasing annealing temperature. Schottky behavior was obtained for the Au/Ni contact deposited after annealed at 400 °C with a clear turn-on voltage around 2.5V and low reverse leakage.

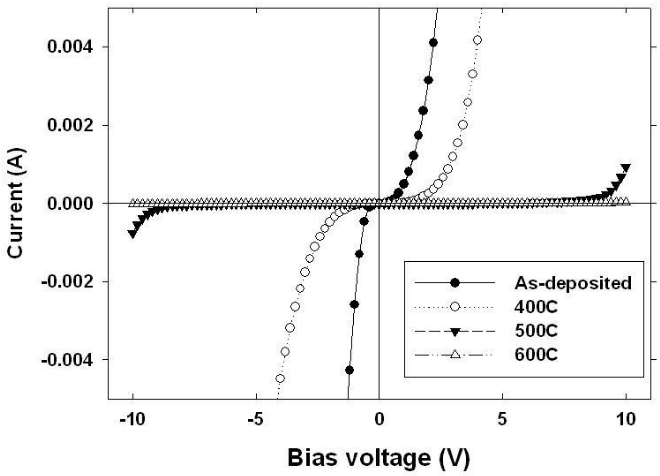

Fig.5. Typical I–V curves of Au/Ni contacts on Al-doped ZnO/p-Si (100) films annealed at different temperatures.

CONCLUSION

In summary, Al-doped ZnO films have been synthesized on silicon substrates by SS-CVD with the substrate temperature of 430°C. The structure of the films remained unaffected by doping.

The energy bandgap value of the undoped ZnO film is 3.24 eV, and the value increases when doped with Al. The optical observations on the films indicate a blue-shift in the absorption edge, improved emission in the UV region.

ACKNOWLEDGEMENT

The authors would like to acknowledge the Universiti Sains Malaysia for financial assistance through a Short Term Grant.

REFERENCES

1. R. H. Wang, J. H. Xin, X. M. Tao, W. A. Daoud, ZnO nanorods grown on cotton fabrics at low temperature. Chem Phys Lett 398 (2004) 250–255.
2. R. H. Wang, J. H. Xin, X. M. Tao, UV-blocking property of dumbbell-shaped ZnO crystallites on cotton fabrics. Inorg Chem 44 (2005) 3926–3930.
3. Y. Wang, C. Ma, X. Sun, H. Li, Preparation of nanocrystalline metal oxide powders with the surfactantmediated method. Inorg Chem Comm 5 (2002) 751–755.
4. S. Basu, P.K. Basu, Nanocrystalline metal oxides for methane sensors: role of noble metals, Journal of Sensors, vol. 2009 (2009) 1-20.
5. B. K. Min and S. D. Choi, SnO_2 thin film gas sensor fabricated by ion beam deposition, Sensors and Actuators B, vol. 98, no. 2-3, (2004) 239–246.
6. M. Jin, J. Feng, Z. De-Heng, M. Hong-Lei, and L. Shu-Ying, Optical and electronic properties of transparent conducting ZnO and ZnO:Al films prepared by evaporating method," Thin Solid Films, vol. 357, no. 2 (1999) 98–101.
7. P. Mitra and A. K. Mukhopadhyay, ZnO thin film as methane sensor, Bulletin of the Polish Academy of Sciences: Technical Sciences, vol. 55, no. 3 (2007) 281–285.
8. P. Bhattacharyya, P. K. Basu, H. Saha, and S. Basu, Fast response methane sensor based on Pd(Ag)/ZnO/Zn MIM structure, Sensor Letters, vol. 4, no. 4 (2006) 371–376.
9. G. Kiriakidis, M. Suchea, S. Christoulakis, N. Katsarakis, Rev. Adv. Mat. Sci. 10 (2005) 215.
10. M. Suchea, K. Christoulakis, N. Moschovis, G. Katsarakis, Thin Solid Films 515 (2006) 551.
11. A.M. Gas'kov, M.N. Rumyantseva, Russ. J. Appl. Chem. 74 (2001) 440.
12. Suchea, S. Christoulakis, N. Katsarakis, T. Kitsopoulos, G. Kiriakidis, Comparative study of zinc oxide and aluminum doped zinc oxide transparent thin films grown by direct current magnetron sputtering, Thin Solid Films 515 (2007) 6562-6566.
13. V. Singh, M. Kumar, R. M. Mehra, A. Wakahara, A. Yoshida, Al-doped zinc oxide thin films by pulsed laser ablation, J. Indian Inst. Sci. 81, (2001) 527-533.
14. martin, J. P. Espinos, A. Justo, J. P. Holgado, F. Yubero, A. R. Gonzalez-Elipe, Preparation of transparent and conductive Al-doped ZnO thin films by ECR plasma enhanced CVD, Surface and Coatings Technology, 151-152 (2002) 289-293.
15. D. Kim, I. Yun, H. Kim, Fabrication of rough Al doped ZnO films deposited by low pressure chemical vapor deposition for high efficiency thin film solar cells, Current Applied Physics 10, (2010) S459-S462.

16. Lennon, R. Kodama, Y. Chang, Y. Sivananthan, M. Despande, Effects of annealing in N2 on sputtered Al-doped ZnO thin films, Journal of vacuum science & technology B: Microelectronics and nanometer structures, 27 (2009) 1641-1645.

17. C.L. Kuo, Y. H. Liang, J. H. Huang, R. C. Wang, J. L. Huang, H. R. Chang, C. P. Liu, Enhanced density control of Al:ZnO nanowires via one-by-one coupling of nanowires and pyramids, J. Nanosci Nanotechnol, 20 (2010) 893-900.

18. F. Wang, H. Chang, C. C. Tseng, C. C. Huang, H. W. Liu, Influence of hydrogen plasma treatment on Al-doped ZnO thin films for amorphous silicon thin film solar cells, Current Applied Physics 11 (2011) S12-S16.

19. Fay, U. Kroll, C. Bucher, E. Vallat-Sauvain, A. Shah, Low pressure chemical vapour deposition of ZnO layers for thin-film solar cells: temperature-induced morphological changes, Sol. Energy Mater. Sol. Cells 86 (2005) 385-397.

20. L.S. Chuah, Z. Hassan, S. S. Tneh, S.G. Teo, "Study of electrical characteristics of ZnO Schottky photodiode on Si substrate", Microelectronics International, 28, 8-11 (2011).

21. L.S. Chuah, Z. Hassan, S.S. Tneh, H. Abu Hassan, "Porous silicon as an intermediate buffer layer for zinc oxide nanorods", Composite Interfaces, 17, 733-742 (2010).

22. L.S. Chuah, Z Hassan, S.S. Tneh, K. G. Saw, S. S. Ng, F. K. Yam, F. Azhari, "The effects of thermal treatments on microstructure phosphorus-doped ZnO layers grown by thermal evaporation", Composite Interfaces, 17, 863-872 (2010).

23. L. S. Chuah, Z. Hassan, S. S. Tneh, "Tetrapod-like ZnO nanostructures deposited on Si substrates with AlN as buffer layer", Composite Interfaces, 18, 49-56 (2011).

24. B.D. Cullity, The Elements of X-Ray Diffraction, Addison–Wesley, Reading, MA, 1978, p. 102.

25. M. Chen, Z.L. Pei, X. Wang, C. Sun, L.S. Wen, J. Vac. Sci. Technol. A 19 (2001) 963.